MAX-PLANCK-INSTITUT FÜR PLASMAPHYSIK

GARCHING BEI MÜNCHEN

Entropy Relaxation of ASDEX Plasmas

FRANK POHL

IPP 6/282 September 1989

Die nachstehende Arbeit wurde im Rahmen des Vertrages zwischen dem Max-Planck-Institut für Plasmaphysik und der Europäischen Atomgemeinschaft über die Zusammenarbeit auf dem Gebiete der Plasmaphysik durchgeführt.

Entropy Relaxation of ASDEX Plasmas

Abstract

In tokamak discharges with improved ohmic confinement (IOC) in ASDEX a transition is observed from flat density profiles towards more peaked ones /4/, while the normalized temperature profile is preserved. For this behaviour of the radial profiles it is shown that the entropy of the plasma increases during the IOC phase. Hence IOC and entropy relaxation are closely related. If the IOC phase is long enough, one finds stationary plasma states, which are compared with the relaxed state described in theory.

Table of Contents

1. Introduction
2. Plasma Entropy
3. Theory of the Relaxed State
4. Technique for $n_e(r,t)$, $T_e(r,t)$ Measurements
5. Entropy Evolution in Different Ohmic Confinement Regimes
6. Comparison with Theory
7. Radial Profiles
8. Relaxation Parameters
9. Summary

Appendix A: Entropy Principle for an Isolated Gas

. . . . Modification of Theory /2/

Appendix B: Computer Program

Appendix C: Safety Factor Ratio

Appendix D: Explanations, Auxiliary Computations etc.

. . . . Re. eq. (1.1) Water Glass Entropy

. . . . Re. eq. (2.2) Entropy per Particle

Acknowledgements, References

1. Introduction

The second law of thermodynamics predicts that temperature differences between interacting parts of a system should relax to zero if certain constraints are satisfied (see Sec. 2 and Appendix A). This process is called "entropy relaxation" because the entropy increases until the temperature difference vanishes. The state with maximum entropy is called the "relaxed state". For example, the entropy of two glasses of water with different temperatures which are isolated from the rest of the universe is approximately of the type

$$S = S_0 - S_1 \, exp(-t/t_{rel}) \tag{1.1}$$

(see Appendix D), where the relaxation time t_{rel} depends on the geometry, length, heat conduction of the glass, specific heat of the water, etc.; S_0 is the entropy of the relaxed state.

Entropy behaviour according to eq. (1.1) is often observed in systems which are not isolated, e. g. in the case of plasmas.

In this paper we investigate the entropy relaxation in tokamak discharges in ASDEX. For this purpose we have to determine the plasma entropy from the radial profiles of the electron density and temperature at different times and look for time intervals in which the plasma entropy is approximately of the "water glass" type in eq. (1.1).

In Sec. 2 we write down the equations for the plasma entropy,
in Sec. 3 we briefly outline the theories of the relaxed state,
in Sec. 4 we describe how the space-time averaged data are obtained for ASDEX,
in Sec. 5 we present the time evolution of the entropy in some ASDEX discharges,
in Sec. 6 we compare the experimental results with the theoretical results of Sec. 2,
in Sec. 7 we present some approximation formulas on radial profiles,
in Sec. 8 we define plasma parameters depending on time similarly to eq. (1.1)
and in the Appendix we present formulas, auxiliary computations and other details.

2. Plasma Entropy

The plasma entropy is

$$S_e = \int_{plasma} d^3x \; n_e \; s_e \tag{2.1}$$

(see Ref. /1/, eq. (4) and our Appendix D), where

$$s_e = s_0 + \frac{ln\,(T_e\; n_e^{1-\gamma})}{\gamma - 1} \tag{2.2}$$

is the entropy per particle of the electron component of the ideal mono atomic plasma gas;
n_e is the electron density;
T_e is the electron temperature;
s_0 is the entropy constant.
For the adiabatic constant we have
$\gamma = 5/3$ if 3 degrees of freedom are assumed,
$\gamma = 2$ if 2 degrees of freedom are assumed.
It will be assumed that $\gamma = 5/3$. (2.3)
The subscript "plasma" in eq. (2.1) stands for the plasma volume $2\pi R\; \pi a^2$;
a is the minor plasma radius;
R is the major radius;
$d^3x = 2\pi R\; 2\pi r\; dr$ is the volume element; (2.4)
r is the radius of the flux surfaces.
All quantities are assumed to depend on space only via r.
Inserting eqs.(1.3-8) in eq. (1.2) gives

$$S_e \sim S_{0e} + \int_0^a dr\; r\; n_e\; ln(T_e n_e^{-2/3}) \; . \tag{2.5}$$

In theoretical work the normalized density and temperature,

$$n = n_e/n_{e0} \; , \qquad T = T_e/T_{e0} \; , \tag{2.6}$$

are used almost exclusively, where
n_{e0} and T_{e0} denote the density and temperature at the centre.
Replacing n_e and T_e by the normalized n and T in the entropy equation (2.5) yields

$$S \sim S_0 + \int_0^a dr\; r\; n\; ln(T\; n^{-2/3}) \; . \tag{2.7}$$

3. Theory of the Relaxed State

In this section we try to determine the "relaxed" state from the entropy principle

$$\delta S = 0 , \tag{3.1}$$

which states that the variation of the plasma entropy in eq. (2.7) must vanish in the relaxed state. Pfirsch has presented two different theories /1/ and /2/ which differ in the constraints on the entropy principle. Both theories have serious disadvantages; in order to avoid theses the author modified theory /2/. Formal details are given in Appendix A. In this section we briefly describe the results and the constraints. We begin with the constraints for an isolated gas.

For an isolated gas we have the constraints

constant volume, (3.2)
constant particle number, (3.3)
constant energy. (3.4)

Introducing these constraints into the entropy principle $\delta S = 0$ yields constant temperature and density (see Appendix A, eqs. (A1-A8)).

Plasmas are, however, not isolated systems. The constraints (3.2) and (3.3) of constant volume and particle number are satisfied in ASDEX plasmas at least in the relaxed state - but there is a serious difference between experiment and theory:
in ASDEX we have a particle flux from sources (gas puff) to sinks (divertor) which may sometimes cause the constraint of constant particle number to be satisfied. Formally, the particle flux would yield additional source terms in /1/, eq. (7) and similarly in theory /2/ and its modification given below. These source terms are neglected: in the theories particles are not allowed to vanish or to be generated.

The constraint (3.4) of constant energy is not satisfied in the plasma case und must be replaced by other constraints. Every theory does this in a different manner.

In his theory /1/ Pfirsch introduces the constraint that the relaxed states
"are characterized by such functions $p(n)$ (p = pressure) for which the entropy no longer changes when the plasma performs arbitrary internal motions which are slow enough so as not to alter the relation between p and n."
The resulting $T(n)$ relation for the relaxed state is

$$T = n^{2/3}\, e^{\alpha - \alpha/n} , \tag{3.5}$$

where α is a constant parameter describing the deviation from the state with constant entropy per particle.

Relation (3.5) has a serious disadvantage: for vanishing density near the plasma boundary the entropy per particle (2.2) becomes singular. We now postulate that the entropy per particle must be regular; hence α is in general no longer constant if we use eq. (3.5) for defining α. Let us write α as a function of the density n. The limit $n = 0$ approximately corresponds to the plasma boundary and the right limit $n = 1$ corresponds to the magnetic centre. Owing to the postulate of regular entropy per particle $\alpha(n)$ must vanish for $n = 0$; hence we have

$$\alpha = c_1 n + c_2 n^2 + \ldots . \tag{3.6}$$

and perhaps terms of the type $n \, ln \, n$, which are neglected because ansatz (3.6) describes with sufficient accuracy the theoretical and experimental data as yet available.
Let us look for theories satisfying postulate (3.6).

In /2/ Pfirsch introduces the constraints

pressure balance	(Ref. /2/, eq. (9))
Spitzer-Ohm-Ampere's law	(Ref. /2/, eq. (14))
variation of the poloidal field and	(Ref. /2/, eq. (24))
variation of the toroidal field.	(Ref. /2/, eq. (25))

The result is radial profiles of temperature, density and magnetic field with the plasma β being the only free parameter. For α we have

$$\alpha(n) \approx 0.4 \, \beta \, n \tag{3.7}$$

(see Ref. /2/, eq. (33)), which satisfies posulate (3.6), where β is the ratio of plasma pressure to magnetic pressure; this means that plasmas with $\beta \leq 0.1$ in the relaxed state are nearly isentropic. This case is not found as yet in ASDEX data investigated by the author.

Let us look for other theories.
In Ref. /1/, Appendix B, we solved for slab geometry the corresponding problem of theory /2/. The result is as follows:
if the poloidal and toroidal fields are varied, as in /2/, we get $T = n^{2/3}$, $\alpha = 0$;
if only the poloidal field is varied and the toroidal field is kept constant, we get relation (3.5) with freely choosable constant parameter α . The addition of the constraint of constant B_z to the constraint of constant particle number treated in /2/ might thus be expected to yield freely choosable α values for circularly cylindrical geometry as well. We therefore

introduce the postulate

$$B_z = B_0 = const \tag{3.8}$$

into theory /2/. The basic equations of this modification are given in Appendix A. The numerical result for α is given in Fig. 1. It can be seen that α has zeros at $n = 1$ and perhaps at $n = 0$.

The zero at $n = 0$ agrees with postulate (3.6) of regular entropy,

the zero at $n = 1$ comes from the radial profiles of density and temperature given by the theory (see eqs. (A20) and (A21)) for small r:

$$T = 1 - 0.10\, r^2 - \ldots \tag{3.9a}$$

and

$$n = 1 - 0.15\, r^2 - \ldots \tag{3.9b}$$

if r is normalized so that

$$B_\phi = \frac{r}{2} - \ldots \tag{3.9c}$$

From eqs. (3.9a-b) we have

$$T = n^{2/3} + \ldots \tag{3.9d}$$

and hence $\alpha = 0$ from eq. (3.5). The entropy per particle (2.2) is constant in second approximation; thus the plasma central region with small r is in higher order isentropic in the relaxed state than in the non-relaxed state when eqs. (3.9) are not satisfied.

Fig. 1
α vs. n
according to theory /2/
modified by introducing
$B_z = B_0$.

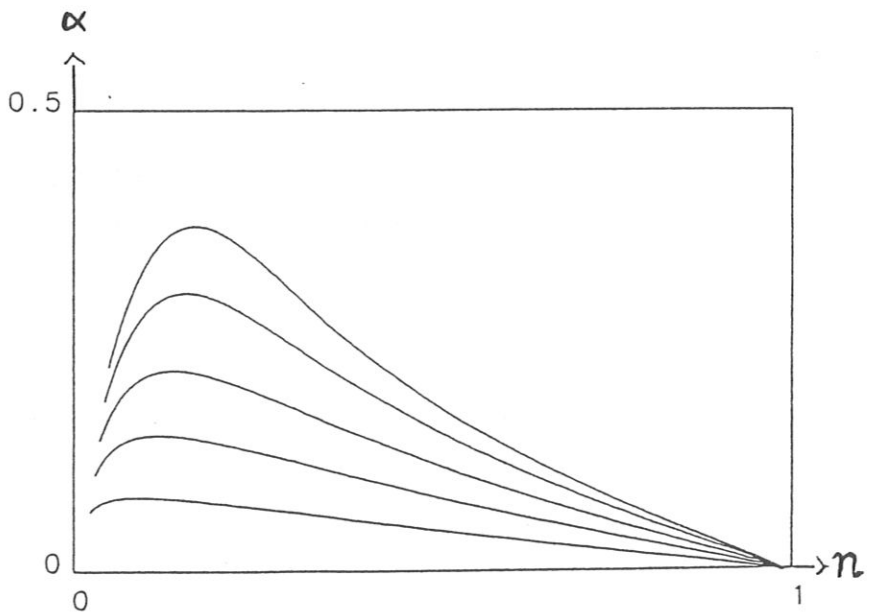

4. Technique for $n_e(r,t)$, $T_e(r,t)$ Measurements

In ASDEX, the plasma density and temperature are measured simultaneously by analyzing Thomson-scattered laser light /3/. This allows theoretical temperature-density relations to be compared with experimental ones. Let us consider Fig. 2, which shows the radial profiles of the density (top) and temperature (bottom) for ASDEX shot no. 23349 at three different times. The numbers 0, 1 and 2 in the plot denote the experimentally measured points, and the dotted curves are profiles fitted with the functions

$$n_e = exp(\, A_{n0} + A_{n1}r^2 + A_{n2}r^4 + A_{n3}r^6) \,, \tag{4.1a}$$

$$T_e = exp(\, A_{T0} + A_{T1}r^2 + A_{T2}r^4 + A_{T3}r^6) \,, \tag{4.1b}$$

r being the radius of the flux surfaces.

Fig. 2

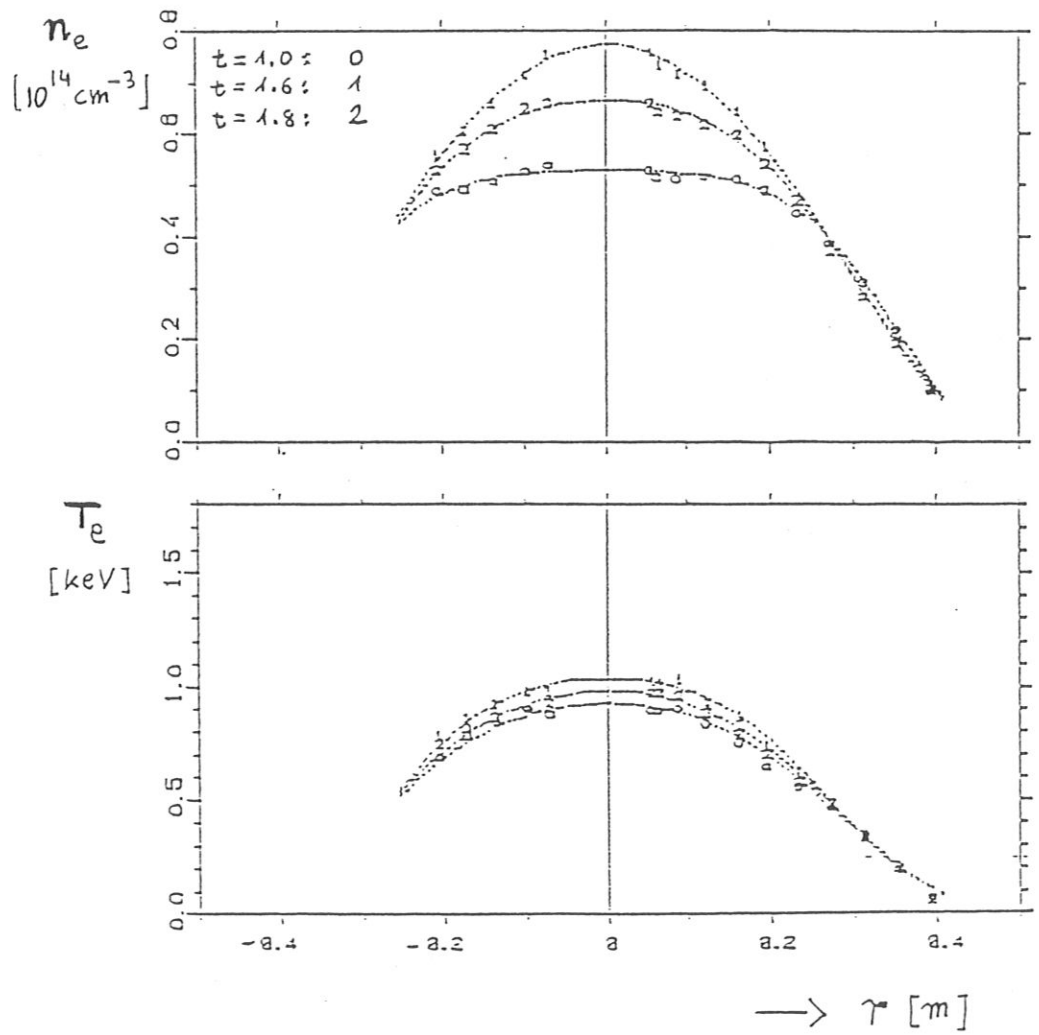

The measurements are made at equidistant times $M\ \Delta t$. The coefficients from eqs. (4.1) are obtained from the signals n_L and T_L by minimizing the error squares

$$Q_n = \sum_{L=1}^{16} \left(A_{n0} + A_{n1}\, r_L^2 + A_{n2}\, r_L^4 + A_{n3}\, r_L^6 - ln\, n_L \right)^2 , \qquad (4.2a)$$

$$Q_T = \sum_{L=1}^{16} \left(A_{T0} + A_{T1}\, r_L^2 + A_{T2}\, r_L^4 + A_{T3}\, r_L^6 - ln\, T_L \right)^2 , \qquad (4.2b)$$

where L denotes the 16 polychromators used for the measurements.
Furthermore, we need time-averaging according to

$$n(r,t) = \frac{1}{2H+1} \sum_{N=M-H}^{M+H} exp\left(A_{n1,N}\, r^2 + A_{n2,N}\, r^4 + A_{n3,N}\, r^6 \right) , \qquad (4.3a)$$

$$T(r,t) = \frac{1}{2H+1} \sum_{N=M-H}^{M+H} exp\left(A_{T1,N}\, r^2 + A_{T2,N}\, r^4 + A_{T3,N}\, r^6 \right) , \qquad (4.3b)$$

where H is approximately the half-length of the time integration interval in units Δt , and
$M =$ time in units Δt .
The difficulty is the choice of the integration interval H :
if H is too small, the inaccuracy is often too great;
if H is too big, the time development itself is averaged away.

In our figures we have $\Delta t = 16\ ms$ and $H = 3$;
hence the total length of the time integration interval is about 0.1 s.
For more details see Appendix B and Ref. /3/.

5. Entropy Evolution in Different Ohmic Confinement Regimes

Recently, a new confinement regime was found for stationary deuterium OH discharges with high densities and peaked density profiles (see Ref. /4/). Let us first characterize the different "regimes" of a discharge by the behaviour of the energy confinement time τ_E with density $\bar{n}_e$:
At small densities τ_E is proportional to $\bar{n}_e$, i.e. we have "linear ohmic confinement" (LOC).
At higher densities τ_E saturates with $\bar{n}_e$. This regime, which is called "saturated ohmic confinement" (SOC), has flat density profiles.
In the same density range a new confinement regime with τ_E again proportional to $\bar{n}_e$ was found. It is called "improved ohmic confinement" (IOC). The density profiles in this regime are more peaked than in SOC.
These confinement regimes are found on ASDEX in the following density ranges:

$$\begin{array}{lll} \tau_E \sim \bar{n}_e & \text{in LOC,} & \bar{n}_e < 0.2\ 10^{14}\ cm^{-3}, \\ \tau_E \approx const & \text{in SOC,} & \bar{n}_e > 0.3\ 10^{14}\ cm^{-3} \ \text{(flat density profiles),} \\ \tau_E \sim \bar{n}_e & \text{in IOC,} & \bar{n}_e > 0.3\ 10^{14}\ cm^{-3} \ \text{(peaked density profiles)} \end{array} \tag{5.1}$$

(see Ref. /4/, FIG. 2). Let us consider some examples.

Figures 2 - 4 show the time development of ASDEX shot no. 23349, which is described in Ref. /4/.

Figure 2 (Ref. /5/) shows the transition from flat density profiles at $t = 1.0\ s$ in the SOC phase to the more peaked density profiles for $t \geq 1.6\ s$ in the IOC phase.

Figure 3 (Ref. /7/) shows the gas flux, plasma current, β_p etc. versus time, furthermore, the entropies

$$S_e = 0.5 + 75. \int_0^a dr\ r\ n_e\ ln(T_e\ n_e^{-2/3}) \tag{5.2}$$

$$S = 1. + 50. \int_0^a dr\ r\ n\ ln(T\ n^{-2/3}) \tag{5.3}$$

(see eqs. (2.5)-(2.7)). The additive constants (0.5 and 1.) and the proportionality factors (75. and 50.) are chosen such that the plots are reasonable for n_e in $10^{14}\ cm^{-3}$ and T_e in keV. The solid and dashed entropy curves are obtained by inserting into eqs. (5.2-3) ASDEX data space-time averaged according to Sec. 4.

The IOC phase begins at $t = 1.17\ s$ (dashed vertical line). (5.4)

Fig. 3
Time evolution of the gas flux, OH power P_{OH} , electron density $\bar{n}_e$,
poloidal β_p and plasma current I_p in OH discharge shot no. 23349.
$I_{p,plateau} = 380\ kA$, $B_t = 2.17\ T$, $q(a) = 2.75$ (5.5)
Bottom:
Entropy S_e (solid), S (dashed) and the approximation

$$S_{app} = 0.5 - exp(\frac{1.16 - t}{0.26}) \qquad 1.3\ s < t < 2.3\ s \tag{5.6}$$

(dotted), which is of the water glass type eq. (1.1). All times are measured in seconds; the time 1.16 s occuring in eq. (5.6) approximately coincides with the begin of the IOC phase.

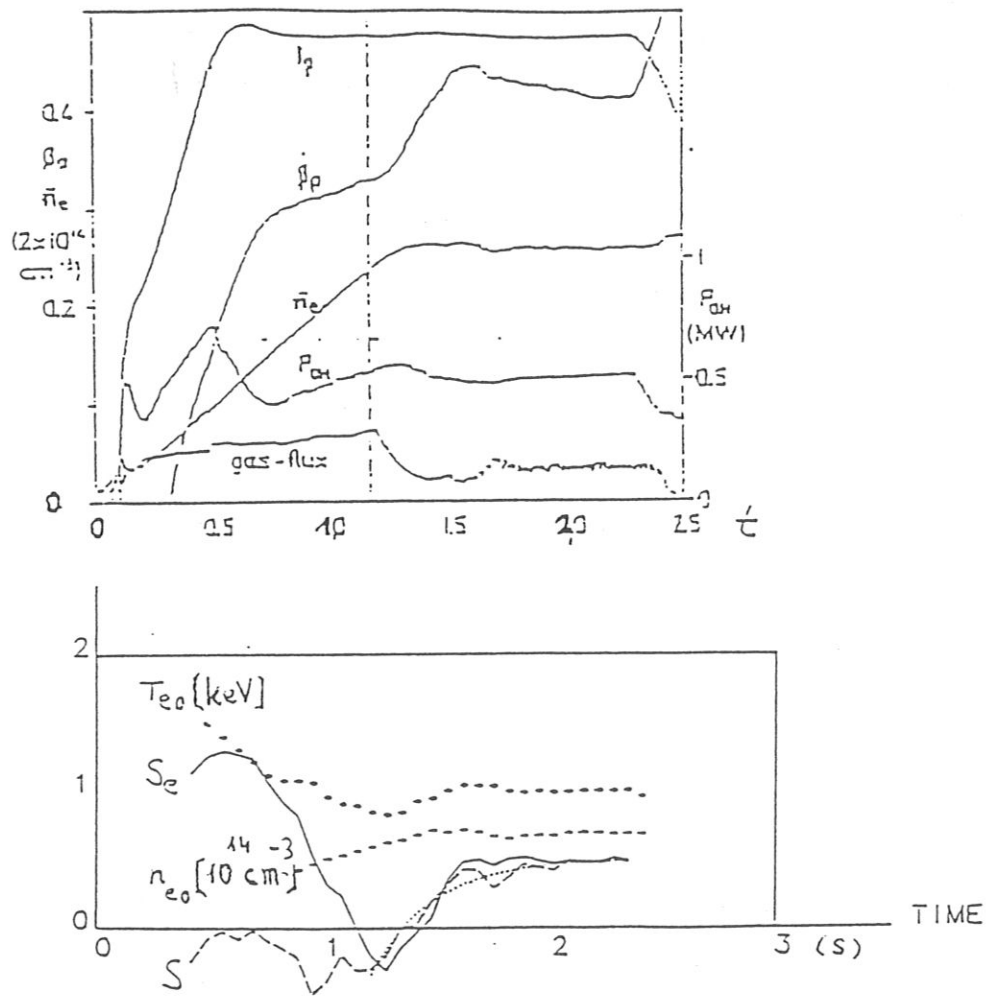

Equation (5.6) is obtained by a least squares fit taking into account the sharp peak of the entropy S near $t = 1.8\ s$ which indicates the change of the sign of the relaxation in the time interval ($1.6\ s < t < 1.8\ s$).This can be seen in Fig. 2, where the density profile is more peaked at $1.6\ s$ than at $1.8\ s$. By neglecting this sharp peak we then have instead of eq. (5.6):

$$S_{app} = 0.5 - exp(\frac{1.33 - t}{0.1}) , \qquad 1.4 < t < 2.3 , \tag{5.7}$$

which approximates the steep increase near $t = 1.4 - 1.5$ better than eq. (5.6). Again all times are given in seconds. The relaxation time $0.1\ s$ is approximately equal to the energy confinement time:

$$t_{rel} \approx \tau_E , \tag{5.8}$$

if the interpretation according to eq. (5.7) is used.
It cannot be determined as yet whether eq. (5.6) or eq. (5.7) is the correct interpretation.

Fig. 4
Entropy S_e (solid), S (dashed), S_{app} (dotted) acc. to eq. (5.7)
for ASDEX shot no. 23349.

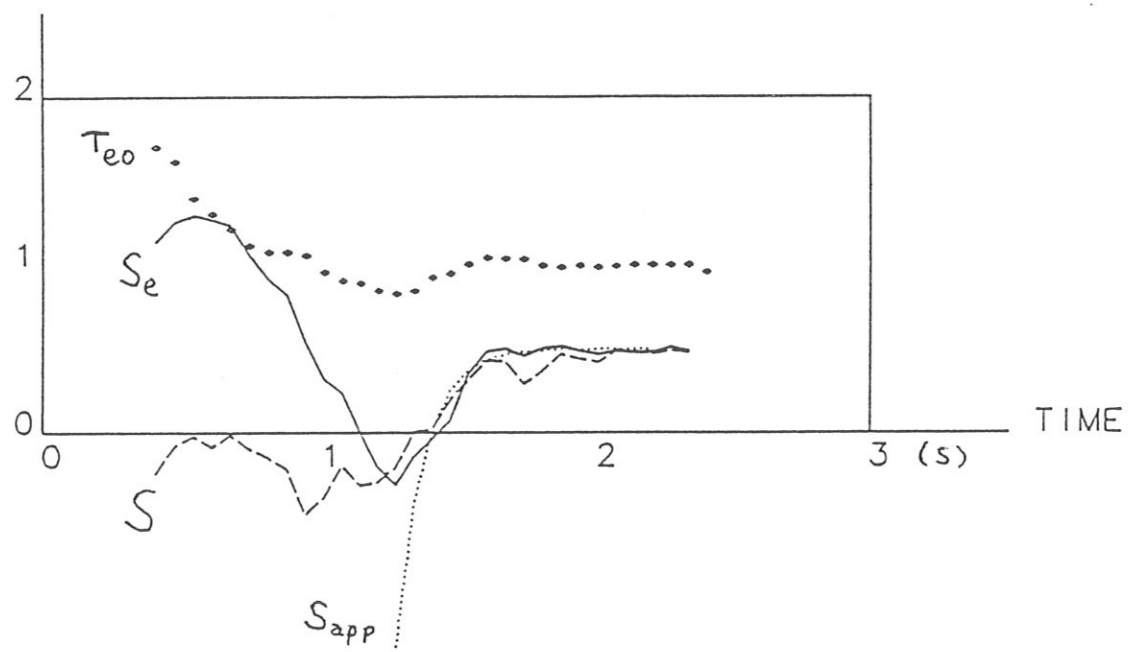

In Fig. 5 we present the time evolution of shot no. 24707 (Ref. /6/). This discharge has two IOC phases with constant density and increasing entropy which are too short for the relaxed state to be reached. It can be seen that the entropy begins to rise after transition to the IOC regime and saturates during both LOC and the stationary IOC phases according to eq. (1.1) with $t_{rel} \approx 0.1 - 0.2\ s$. This may be interpreted as entropy relaxation. - In contrast, during SOC the entropy decreases.

Fig. 5
shot no.
24707
plotted
analogously
to Fig. 3

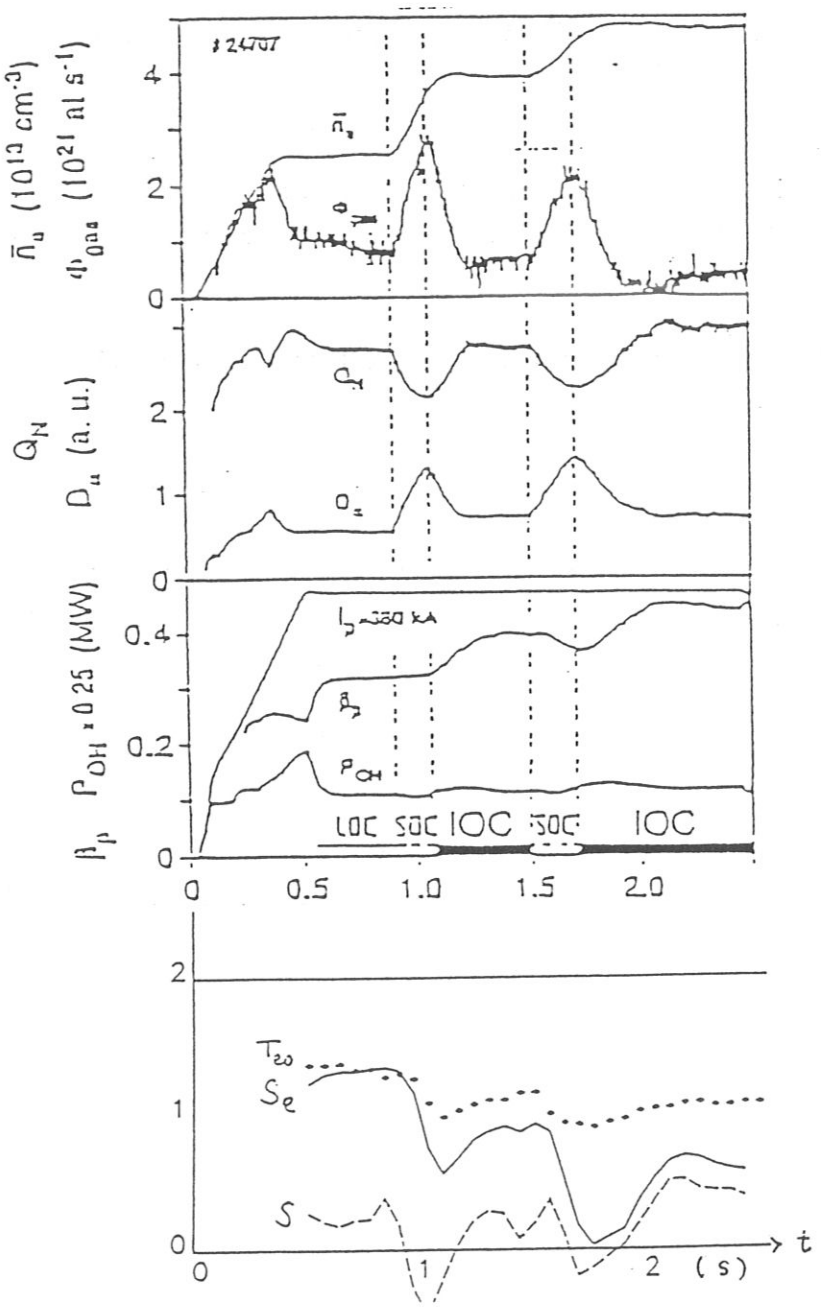

Figure 6 presents a discharge without IOC:
in shot 24147 (Ref. /8/) the continuous, high gas flux from the wall after carbonization prevents the IOC transition; hence the discharge remains in the SOC regime at high densities. It can be seen that the entropy decreases as observed in the SOC phase of the preceding shots (see Figs. 3 - 5)). The entropy does not, however, increase again, as is typical of IOC phases, but saturates at a low value.

Considering Figs. 3-6 one finds that the entropy strongly increases only in the IOC regime.

Fig. 6
T_{e0} , n_{e0} , S_e and S vs. t

analogously to Figs. 3 and 4; perhaps entropy relaxation for $t > 2$.

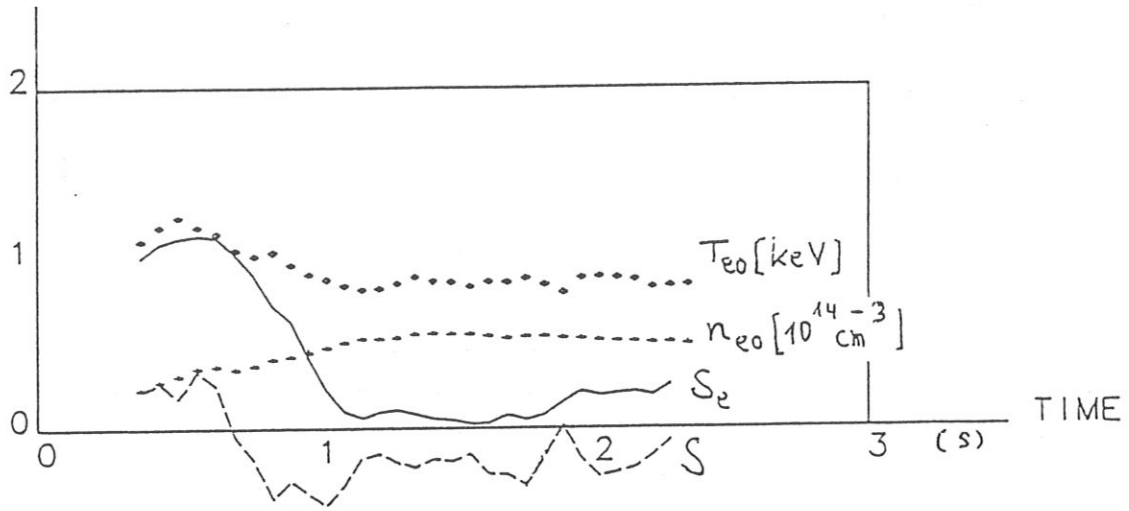

6. Comparison with Theory

The theories presented in Sec. 3 yield α as a function of the normalized density. In order to check the theoretical results against ASDEX data, we resolve eq. (3.5) with respect to α,

$$\alpha = \frac{ln\ (T\ n^{-2/3})}{1\ -\ 1/n} \tag{6.1}$$

and insert the space-time averaged radial profiles into the right-hand side of eq. (6.1). This yields the solid curves in Fig. 7 , which are called "experimental α".

Theories are only available for the relaxed state. The results of the foregoing section indicate that the relaxed state might be the steady-state phase of the IOC regime found in, for example, shot 23349 for $t > 1.6\ s$. Let us therefore consider α vs. n at various times as shown in Fig. 7. It can be seen that the time evolution of α runs

slowly for $t < 1.4\ s$,
quickly near $t = 1.4-1.5\ s$, (6.2)
slowly for $t > 1.6\ s$.

For $t > 1.4\ s$ except $1.7 < t < 1.9$ (see interpretation (5.7)) α can be described by

$$\alpha \approx\ \alpha_{ap}\ =\ 1.3\ (n - n^2)\ +\ n^2\ exp\left(\frac{1.45 - t}{0.12}\right) \tag{6.3}$$

(dashed in Fig. 7), which can be obtained from the experimental α (solid) by cut-off expansion (3.6) after the second-order term and a least squares fit described in Appendix B for the coefficients c_1 and c_2 as functions of time. c_1 is found to be approximately constant and c_2 to be approximately of the water glass type (1.1):

$$c_1(t) \approx c_{1ap} = c\ , \qquad\qquad c_2(t) \approx c_{2ap} =\ -\ c\ +\ c\ exp\left(\frac{\hat{t}_0 - t}{t_{relax}}\right)\ . \tag{6.4}$$

The coefficient c describes the deviation from isentropy in the relaxed state in eq. (6.5); see below.
The relaxation time $t_r = 0.12\ s$ is approximately the energy confinement time for IOC; see FIG. 2 in /4/;
the time $t_0 = 1.45\ s$ with maximal increase of the entropy is approximately the limit of the range of validity for the water glass entropy, if interpretation (5.7) is used.

The relaxed state is defined by very large t; in this case we have

$$\alpha_{ap}\ =\ c\ (n\ -\ n^2) \qquad with \qquad c\ \approx\ 1.3\ . \tag{6.5}$$

Equation (6.5) is approximately the experimental result, which we have to compare with theoretical ones. In Sec. 2 no $\alpha(n)$ similar to the parabola (6.5) is found. The modified

theory predicts the two zeros of $\alpha(n)$ at $n = 0$ and $n = 1$, but is only valid in the central region, where the assumption of constant toroidal magnetic field is at least approximately valid. For other shots with long IOC intervals the $\alpha(n)$ diagrams look similar to those in Fig. 7.

Fig. 7
α vs. n during entropy relaxation for ASDEX shot no. 23349:
solid: $\alpha(n)$ as taken from the experimental data,
dashed: $\alpha_{ap}(n)$ according to

$$\alpha_{ap} = 1.34\,(n - n^2) + exp(\frac{1.45 - t}{0.12}), \quad t \gtrsim 1.4\ s\ , \qquad (6.3)$$

for the times $t = 1.0$, 1.1 , 1.3 , 1.4 , 1.5 , 1.6 , 2.03 s.
Interpretation (5.7) is used; $t = 1.8$ is omitted.

Approximation (5.3)
is of no use
for $t = 1.3\ s$.

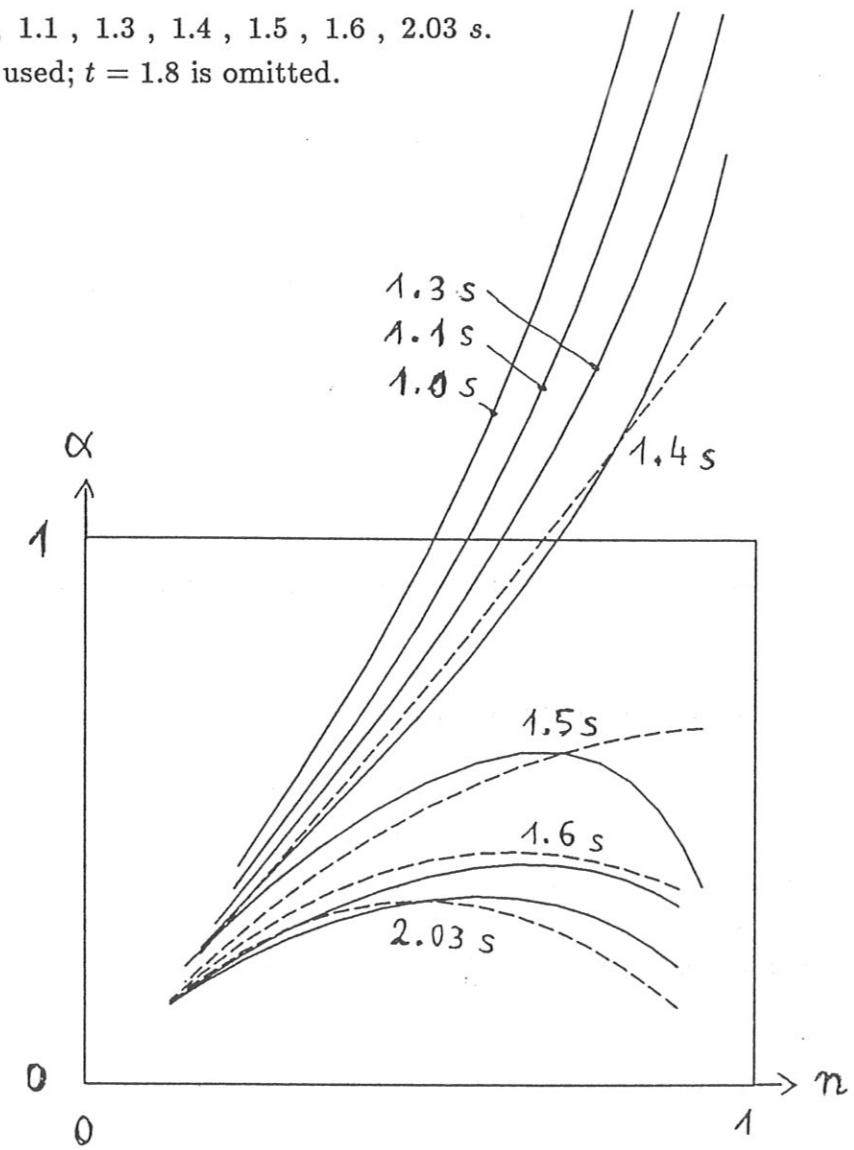

Fig. 8 shows T versus n for ASDEX shot no. 23349 at the same times as in Fig. 7; the dashed curves are obtained by inserting approximation (6.3) into eq. (3.5).
$T = n^{2/3}$ is the isentropic case.

Fig. 8

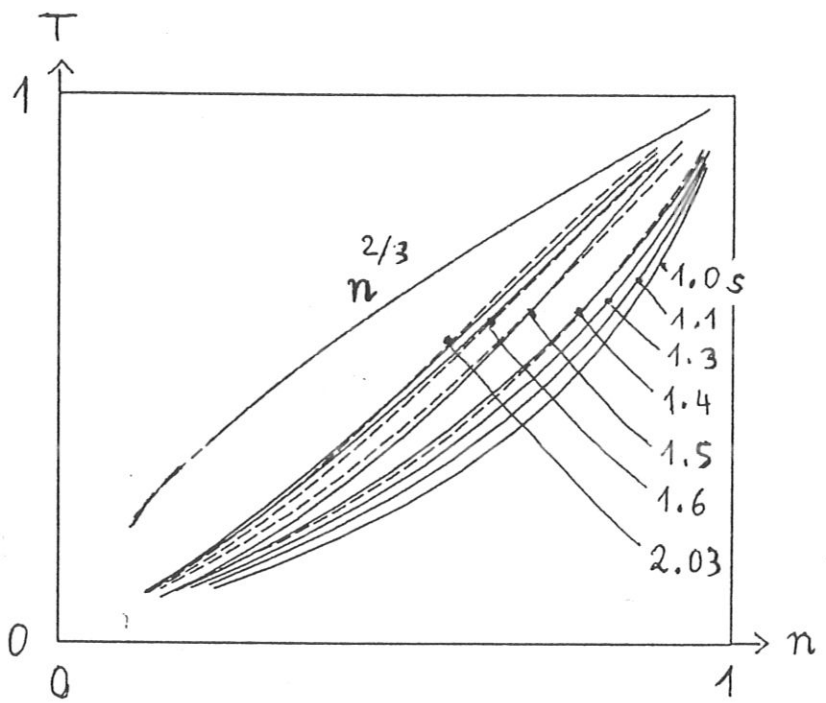

The results can be given in the form of the following table, α being defined in eq. (3.5).

Table 6
$\alpha(n)$ for various theories and experiments

theory /1/:	$\alpha = c_0 = const$	s. (3.5)
theory /2/:	$\alpha = c_1 n$	(3.7)
regular entropy per particle:	$\alpha = c_1 n + c_2 n^2 + \ldots .$	(3.6)
relaxed state, schematic:	$\alpha = c_1 n (1-n)$	(6.5)
ASDEX shot 23349, $t = 2.0$ s:	$\alpha = 1.2 n - 1.1 n^2$	

7. Radial Profiles

In this section we describe the radial profiles of the normalized electron density and temperature by approximation formulas which contain a time-dependent parameter causing the plasma entropy to be of the water glass type (1.1).

The density is approximated by

$$n_a \;=\; 1 \;-\; \hat{r}^E \;+\; 0.1\,\hat{r}^{12}\;, \qquad \hat{r} = r/a \tag{7.1a}$$

with

$$E \;=\; 2 \;+\; exp\left(\frac{\tilde{t}_0 - t}{t_r}\right)\;, \qquad t > t_L; \tag{7.1b}$$

Equations (7.1a), (7.3) and (7.4) (below) hold more or less well in all discharges at almost all times,
eq. (7.1b) only in IOC phases;
$t_L \approx t_0$ limits the range of validity for eq. (7.1b);
t_r is the relaxation time and is approximately equal to the the energy confinement time if interpretation (5.7) is used.
The time evolution of the exponent E describes the transition from flat profiles at the beginning of the IOC phase towards more peaked ones later ;
the term $0.1\,\hat{r}^{12}$ approximates the density near the plasma boundary.
In the case of radial profiles of ASDEX shot no. 23349 taken at the times 1.0 , 1.1 , 1.3 , 1.4 , 1.5 , 1.6 and 2.03 s interpretation (5.7) is suitable with

$$t_L = \tilde{t}_0 = 1.4\ s\;, \qquad t_r = 0.1\ s\;. \tag{7.2}$$

The normalized temperature is approximately

$$T_a \;=\; exp(-2.4\,\hat{r}^3) \tag{7.3}$$

independently of time (tested for $t > 0.7\ s$).
Inserting eqs. (7.1a) and (7.3) into eq. (5.3) for the plasma entropy yields with an inaccuracy of about 0.003 for $1 \le E \le 4$

$$S_a \;=\; 1 \;+\; 8\int_0^1 d\hat{r}\;\hat{r}\;n_a\;ln(T_a\;n_a^{-2/3}) \;=\; 0.5\left(\;3 - E \;+\; 0.1\;(E-2)^2\right)\;. \tag{7.4}$$

Equation (7.4) correlates entropy relaxation with the time evolution of the radial profiles at almost all times, not only in IOC phases. In IOC linearization of eq. (7.4) gives together with eq. (7.1b) the water glass entropy of eq. (1.1) with $t_{rel} = t_r$.

In the following figures we compare ASDEX radial profiles space-time averaged according to Sec. 4 (solid) with the approximation formulas (dashed).

Fig. 9
Radial density profiles
solid: space-time averaged data from ASDEX shot no. 23349
at the times 1.0 , 1.1 , 1.3 , 1.4 , 1.5 , 1.6 and 2.03 s;
dashed: according to the approximation formulas (7.1a), (7.1b) and the data given in (7.2).
The plot of n_a is omitted for $t \leq 1.3$ because $t \leq 1.3$ is outside the range of validity of eq. (7.1b); the solid curves for $t = 1.6$ and $t = 2.03$ coincide.

The approximations (7.1-2) show the transition from flat profiles for $t \leq 1.3$ towards more peaked ones for $t \geq 1.6$ s by varying the exponent E in eq. (7.1b) from about 3 to 2.

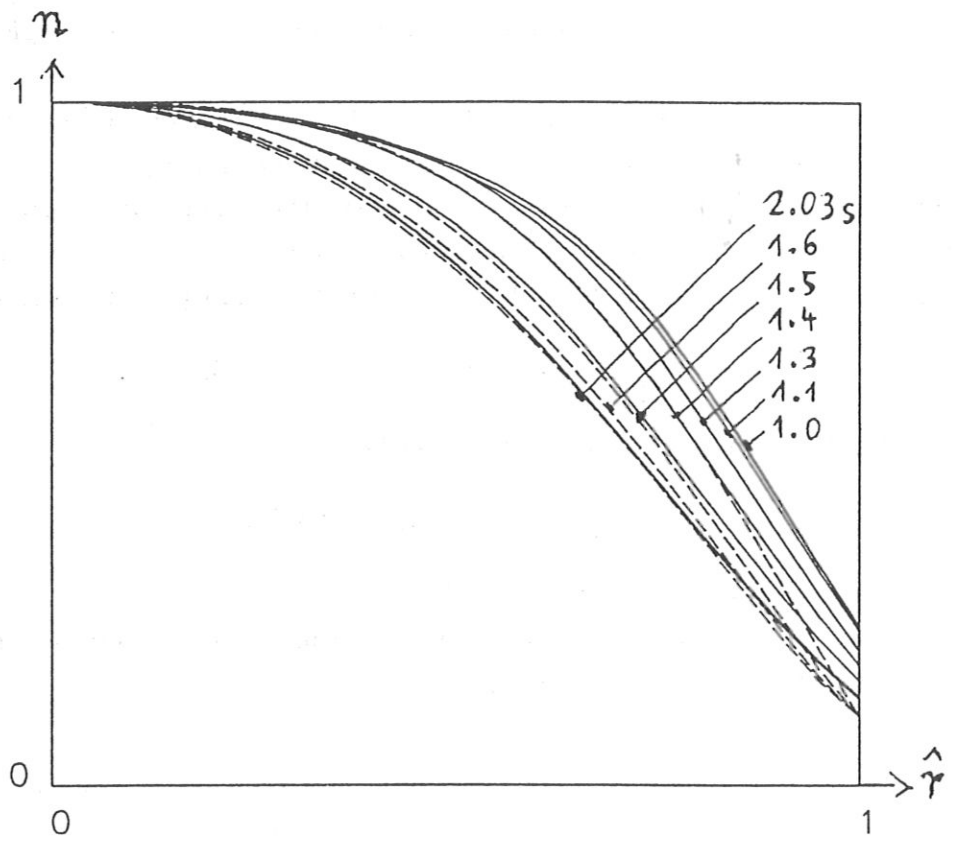

Fig. 10
Radial temperature profiles
dashed: $T_a = exp(-2.4\ \hat{r}^3)$ (7.3)
solid: space-time averaged data from ASDEX shot no. 23349
at the times 1.0 , 1.1 , 1.3 , 1.4 , 1.5 , 1.6 and 2.03 s;

Approximation eq. (7.3) does not yield the behaviour for small r:
in the relaxed state we have $T = 1 - 0.66\ \hat{r}^2 - \ \ldots$
from eqs. (3.9a-b) and (7.1-2).

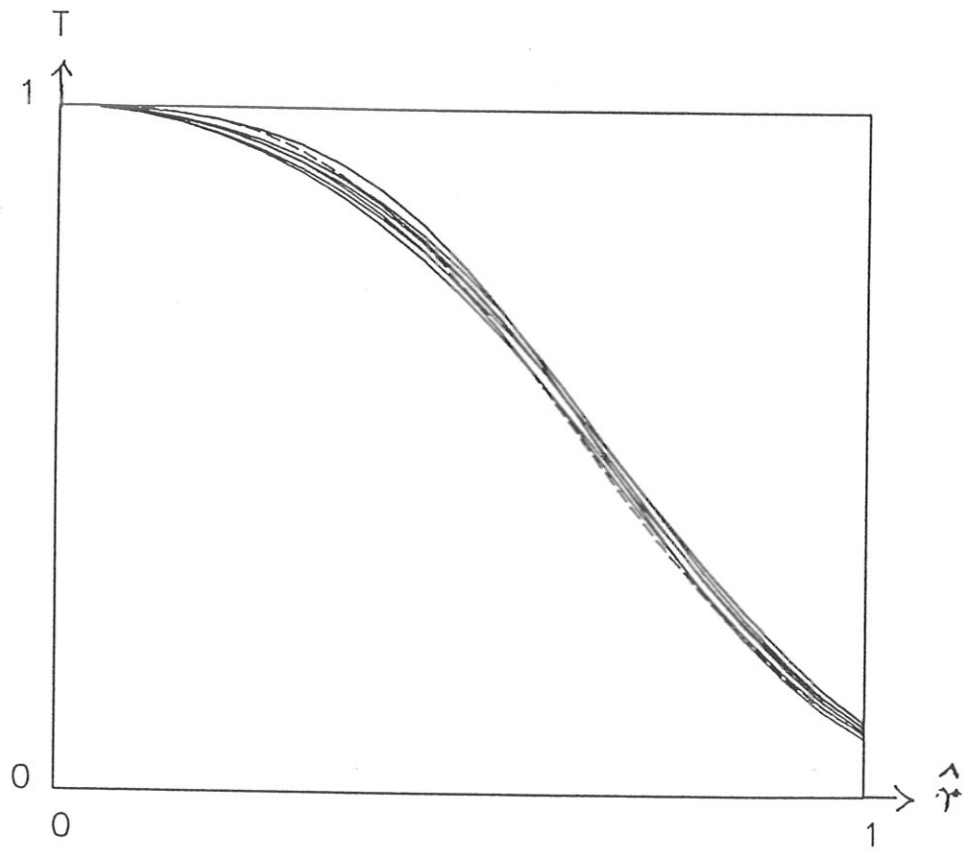

Also in other shots the normalized temperature is approximately constant:

Fig. 11
Radial temperature profiles
dashed: $T_a = exp(-1.9\ R^{2.5})$ (7.5)
solid: space-time averaged data from ASDEX shot no. 24147 (see Fig. 6)
at the times 1.1 , 1.4 , 1.7 , 2.0 and 2.3 s.

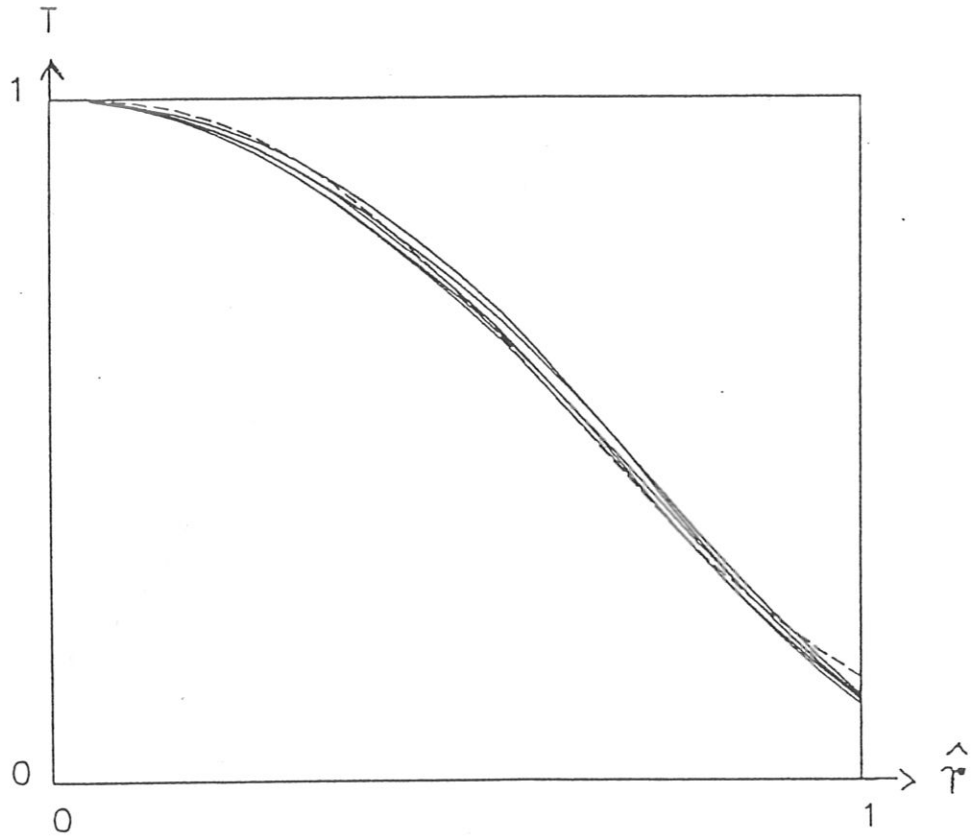

Equations (7.3) and (7.5) are special cases of the more general rule

$$T \approx T_a = exp(- \frac{2}{3} U R^V) , \tag{7.6}$$

with U, V being time-independent parameters. Equation (7.6) also contains Coppi's Gauss temperature /9/ as the special case $V = 2$, where U is essentially the safety factor ratio. In our Appendix C we determine the safety factor ratio for the more general case in eq. (7.6). The result is

$$\frac{q_a}{q_0} \approx \frac{U^C}{\Pi(C)} \frac{P}{1 - e^{-P}} \tag{7.7}$$

with

$$C = \frac{2}{V} - 1 , \qquad P = \frac{1}{2} U V , \tag{7.8}$$

and with $\Pi(C) = \Gamma(C + 1)$ being the factorial.
Inserting the values $U = 2.4$ and $V = 3$ of shot no. 23349 (see eq. (7.3)) yields

$$\frac{q_a}{q_0} \approx 2.6 , \tag{7.9}$$

which approximately agrees with $q_a/q_0 = 2.75$ given in eq. (5.5) in connection with Fig. 3. Most shots have V values of about 2.8.

8. Relaxation Parameters

Looking at the preceding sections, one finds besides the plasma entropy two parameters depending on time similarly to the water glass entropy in eq. (1.1), namely the parameter c_2 occuring in eq. (6.4) and the exponent E describing the time evolution of the radial density profiles (see eqs. (7.1)). From these we define so-called "relaxation parameters" with approximately equal time behaviour.

In order to do this we linearize eq. (7.4)

$$1 - 2\,S_a = E - 2 \tag{8.1}$$

and resolve eq. (7.1a) for E by integrating over $\hat{r}$ from 0 to 1:

$$E = \frac{F_a}{1 - F_a}, \qquad F_a = \frac{0.1}{13} + \int_0^1 n_a \, d\hat{r} \; . \tag{8.2}$$

Now we replace in eq. (8.1-2) S_a by S and n_a by n and define the left-hand side of eq. (8.1) by U_S :

$$U_S = 1 - 2\,S \tag{8.3}$$

and the right-hand side of eq. (8.1) by U_E :

$$U_E = \frac{F}{1 - F} - 2\,, \qquad F = \frac{0.1}{13} + \int_0^1 n \, d\hat{r} \; . \tag{8.4}$$

Furthermore, we define

$$U_C = \frac{c_1 + c_2}{c_1}\,, \tag{8.5}$$

where c_1 and c_2 are obtained by the least squares fit as described in Appendix B. We expect from eqs. (5.7), (6.4), (7.1b), (7.2) and (8.1) that

$$U_S \approx U_E \approx U_C \approx U_A = exp\left(\frac{t_0 - t}{t_R}\right) \qquad t \geq t_0 \tag{8.6}$$

describe at least in crude approximation the entropy relaxation in sufficient long IOC phases; U_S , U_E , U_C and U_A are the "relaxation parameters" mentioned above; furthermore, we use in the plots the arithmetic mean

$$U_M = \frac{1}{3}\,(U_S + U_E + U_C) \; . \tag{8.7}$$

Equations (8.6) denote three more or less well-satisfied relations and one definition, namely

$$U_A \;=\; exp\left(\frac{t_0 - t}{t_R}\right) , \qquad (8.6a)$$

describing entropy relaxation of water glass type. Let us discuss the very different ranges of validity occuring in eqs. (8.6). The relation

$$U_S \approx U_A \qquad for \quad t \geq t_0 \qquad (8.6b)$$

means relaxation of the plasma entropy analogously to the entropy (1.1) of water glasses, which is often observed in the IOC regime of ASDEX discharges. The interpretation may be that the plasma relaxes more or less undisturbed towards the state with largest probability and entropy. For $t < t_0$ relation (8.6b) fails; this might have to do with external influences causing the entropy to decrease or to increase slowly as compared with eq. (8.6b). - The relation

$$U_S \approx U_E \qquad or \qquad 1 \;-\; 2\,S \;\approx\; E \;-\; 2 \qquad (8.6c)$$

correlates the entropy with the exponent E of the radial density profile and has a much larger range of validity including also SOC and other regimes, except some small time intervals with "exotic" profiles.

The parameter U_C shows much more irregularities than U_E and U_S; this has to do with fact that
U_C contains two parameters c_1, c_2 defined by a least squares fit which is sensitive against inaccuracies, while
U_E and U_S depend on only one parameter (F in the case of U_E and S in the case of U_S) , which are much less sensitive against inaccuracies.

Figures 12 , 13 and 14 show examples:
In the case of ASDEX shot no. 23349 (Fig. 12) the relaxation parameters coincide fairly well and go to zero according to

$$U_A \;=\; exp\left(\frac{1.4 - t}{0.1}\right) \qquad for \quad t \geq 1.4\ s \qquad (8.8a)$$

for $t \geq 2\ s$ the plasma state becomes relaxed.

At the end of the discharge shot no. 24707 (Fig. 13) the parameter U_C has strongly decreased but not to zero. The interpretation is that the IOC phase is too short to become a relaxed plasma state. Furthermore, the c_1 , c_2 computation breaks down near $t = 1\ s$. For U_A we chose

$$U_A \;=\; exp\left(\frac{1.9 - t}{0.2}\right) \qquad t \geq 1.9\ s \qquad (8.8b)$$

Fig. 12
Top: relaxation parameters U_E (solid) , U_S (dashed) and U_c (dotted) vs. time;
bottom: U_A according to interpretation (5.7)

$$U_A = exp\left(\frac{1.4 - t}{0.1}\right) \tag{8.8a}$$

and the arithmetic mean

$$U_M = \frac{1}{3}\,(U_S + U_E + U_c) \tag{8.7}$$

vs. time for ASDEX shot no. 23349

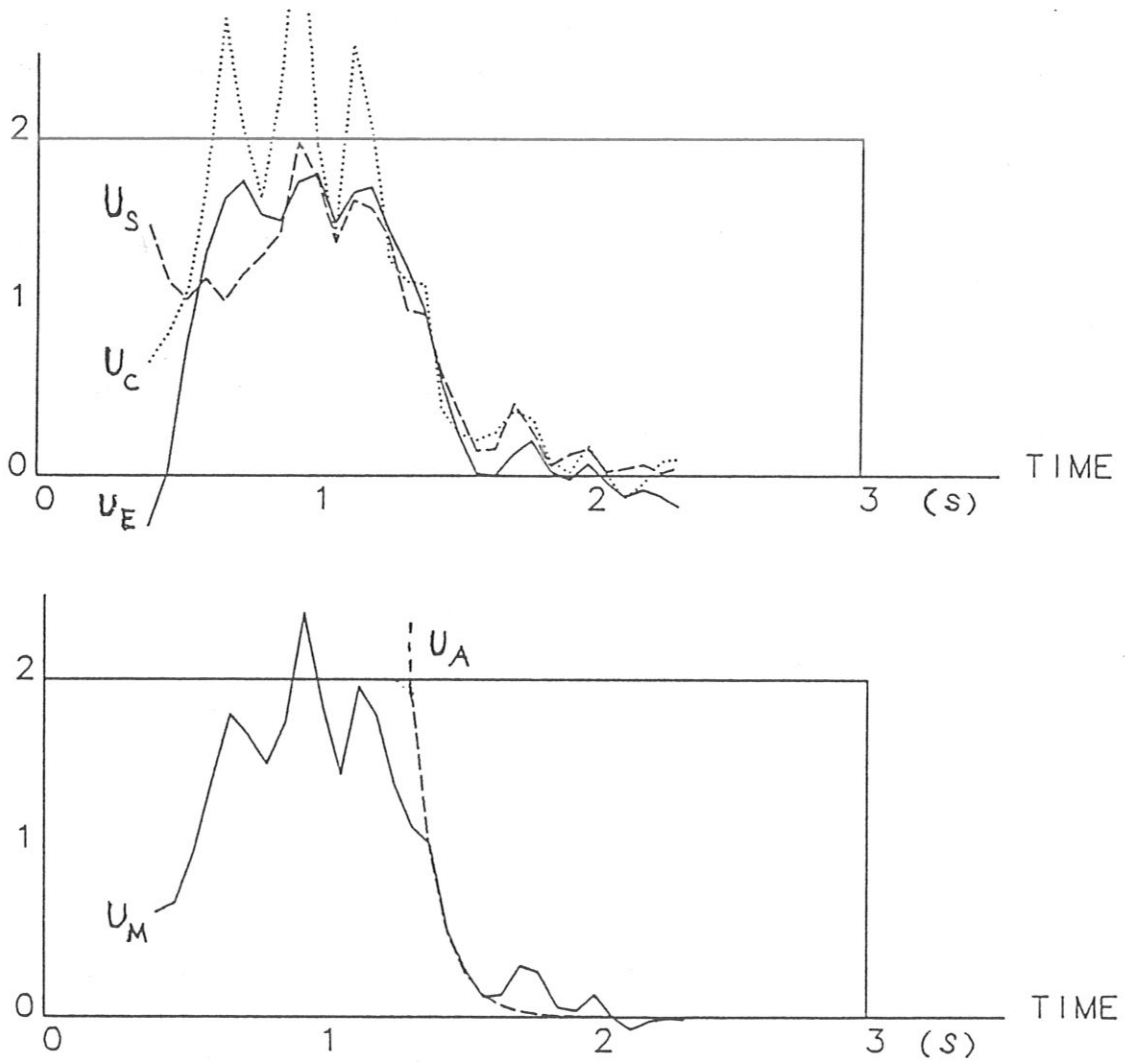

Fig. 13

Top: relaxation parameters U_E (solid) , U_S (dashed) and U_c (dotted) vs. time;
bottom: U_A according to

$$U_A = exp\left(\frac{1.9 - t}{0.2}\right) \tag{8.8b}$$

and the arithmetic mean U_M (see eq. (8.7) vs. time for ASDEX shot no. 24707

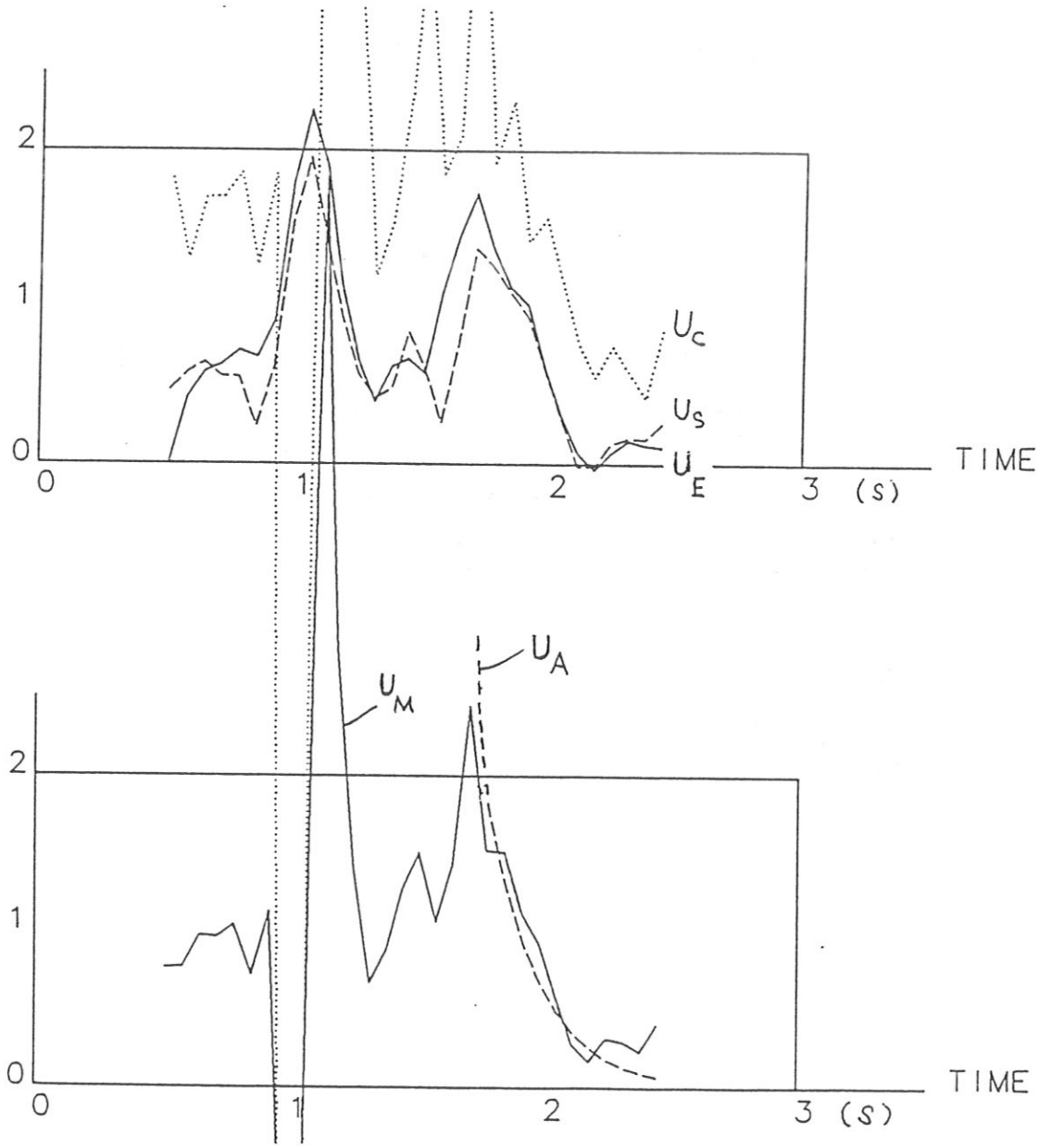

Fig 14 shows the relaxation parameters for shot no. 24147 (see Fig. 6). This discharge remains in SOC; all relaxation parameters are far from zero. Thus we have the rules:

Strong decrease of the relaxation parameters $->$ IOC

Saturating of the relaxation parameters near zero $->$ relaxed state, stationary IOC

No strong decrease of the relaxation parameters $->$ No IOC.

Fig. 14
Relaxation parameters U_E (solid) , U_S (dashed) and U_c (dotted) vs. time

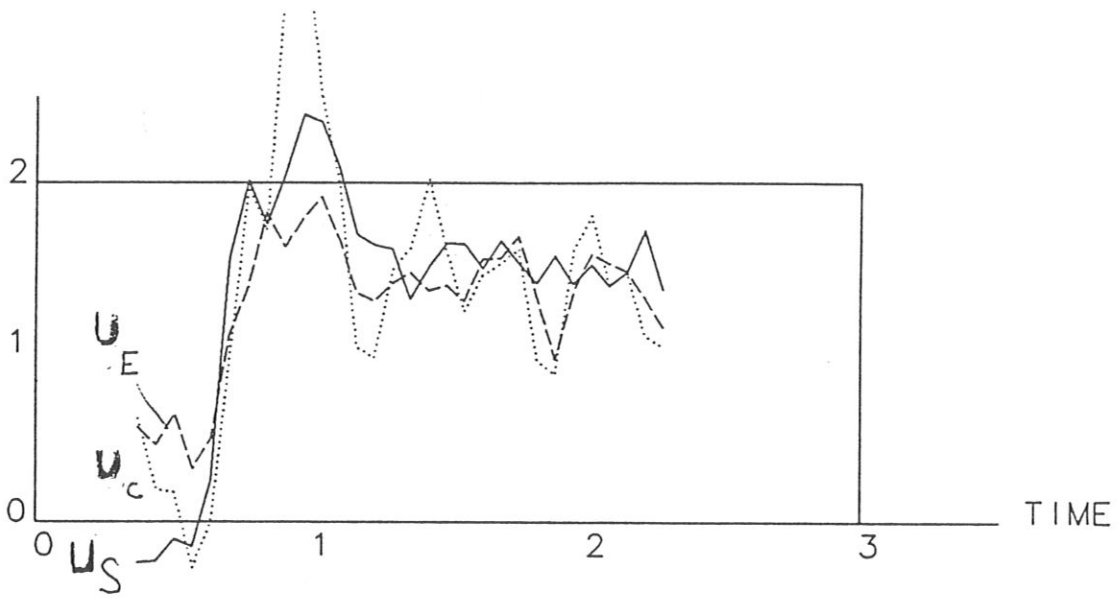

8. Summary

In the IOC regime of ohmically heated discharges on ASDEX the plasma entropy is found to behave similarly to the entropy of an isolated thermodynamic system with regions of different temperatures relaxing towards equilibrium. This is interpreted as "entropy relaxation". Theories of the relaxed state are checked against ASDEX data; theory /2/ was modified. The modified theory yields the radial profiles of the normalized density and temperature in the relaxed state for small r and predicts

$$\alpha(n=0) \;=\; \alpha(n=1) \;=\; 0.$$

The experimental data suggest that $\alpha(n)$ should be approximately the parabola

$$\alpha \;\sim n\,(1-n)\;, \qquad (s.6.5)$$

n is the normalized electron density.

Besides the entropy S itself, there are two other parameters which depend on time similarly to the water glass entropy in eq. (1.1): the parameter c_2 from the α expansion and the exponent E describing the time evolution of the radial density profiles,

$$n_a = 1 - \hat{r}^E \;+\; \ldots\,, \qquad \hat{r} = r/a\;, \qquad (s.7.1a)$$

while the normalized temperature remains approximately constant near

$$T_a \;=\; exp(-2.4\,\hat{r}^3)\;. \qquad (s.7.3)$$

From this behaviour of the radial profiles and the equations for the entropy we have

$$1 \;-\; 2\,S \;\approx\; E \;-\; 2 \qquad (s.8.6c)$$

correlating the relaxation of the entropy S and the profile evolution described by E.
From S, c_2 and E we constructed so-called "relaxation parameters" (see Sec. 8), which coincide well in the case of ASDEX shot no. 23349 and less well in the case of ASDEX shot no. 24707. All relaxation parameters decrease in the IOC phases, sometimes towards zero, which indicates the relaxed state, as in shot no. 23349.
The entropy increases in the IOC regime; if the IOC phase is long enough, the entropy saturates; the stationary IOC regime is the relaxed state with maximum entropy.

Appendix A: Entropy Principle for an Isolated Gas

The entropy is a thermodynamic potential if the energy, the particle number N and volume V are taken as thermodynamic variables. The constraints

$$energy = \int_V p\, dV = const\,, \tag{A1}$$

$$N = \int_V n\, dV = const\,, \tag{A2}$$

$$V = const \tag{A3}$$

define an "isolated system", e.g., an isolated gas-containing box. The entropy principle defining the relaxed state reads for this case

$$\delta \int_V \left(n\, ln\, (p\, n^{-\gamma}) + \lambda\, n + \mu\, p \right) dV = 0\,, \tag{A4}$$

where the first term

$$n\, ln\, (p\, n^{-\gamma}) = n\, (\gamma - 1)\, (s - s_0)\,; \tag{A5}$$

$\gamma = 5/3$ is the adiabatic constant for the ideal plasma gas;
λ contains the entropy constant and the Lagrange multiplier arising from the constraint (A2) of constant particle number;
μ is the Lagrange multiplier arising from the constraint (A1) of constant energy.

Let n and p describe the relaxed state and δp a small deviation. We then have

$$\delta \int_V \left(n\, ln\, (p\, n^{-\gamma}) + \lambda\, n + \mu\, p \right) dV$$

$$= \int_V \left(n\, \frac{\delta p}{p} + \mu\, \delta p \right) dV = 0.$$

This must hold for every choice of δp at every point of the volume; hence the integrand must vanish:

$$\frac{n}{p} = \frac{1}{T} = -\mu = const; \tag{A6}$$

hence the temperature is constant. - Analogously, for a small density variation we have

$$\delta \int_V \left(n\, ln\, (p\, n^{-\gamma}) + \lambda\, n + \mu\, p \right) dV = \int_V \delta n \left(ln\, (p\, n^{-\gamma}) - \gamma + \lambda \right) dV = 0. \tag{A7}$$

This must hold for every choice of δn at every point of the volume; hence the integrand must vanish:

$$ln(p\ n^{-\gamma}) \ = \ ln(T\ n^{1-\gamma}) \ = \ \gamma - \lambda = \ const. \qquad (A8)$$

T is constant, hence from eq. (A8) n also.

Modification of Theory /2/

As already discussed in Sec. 2, we introduce the postulate

$$B_z \ = \ B_0 \ = \ const \qquad (A9)$$

into theory /2/. We now have to determine the quantities p , T , B_ϕ from the three equations
pressure balance

$$p \ = \ 1. \ - \ \frac{1}{2}\ B_\phi^2 \ - \ \int_0^r \frac{dr'}{r'} B_\phi^2 \qquad (A10)$$

(see Ref. /2/, eq. (9)),
Spitzer-Ohm-Ampere law

$$T^{3/2} \ = \ \frac{1}{r}\ \frac{d}{dr}(r\ B_\phi) \qquad (A11)$$

(see Ref. /2/, eq. (14)),
and the entropy principle

$$\delta \int_0^a dr\ r\ L \ = \ \int_0^a dr\ r \left(\frac{\partial L}{\partial p}\ \delta p \ + \ \frac{\partial L}{\partial T^{3/2}}\ \delta T^{3/2} \right) \ = \ 0\ , \qquad (A12)$$

with

$$L \ = \ \frac{p}{T} \left(- \ \frac{2}{3}\ ln\ p \ + \ \frac{5}{3}\ ln\ T \ + \ \mu_1 \right) \qquad (A13)$$

being proportional to the entropy per volume; μ_1 is a constant parameter containing the entropy constant and the Lagrange multiplier arising from the constraint of constant particle number.

In eq. (A12) only B_ϕ is varied; δp and $\delta T^{3/2}$ can be expressed by δB_ϕ via eqs. (A10 and A11) to yield

$$\frac{d}{dr}\ \frac{\partial L}{\partial T^{3/2}} \ = \ B_\phi \left(- \ \frac{\partial L}{\partial p} \ + \ \frac{2}{r^2} \int_0^r dr'\ r'\ \frac{\partial L}{\partial p}\bigg|_{r'} \right) \qquad (A14)$$

(see Ref. /2/, eq. (24));. δB_ϕ drops out similarly to δp and δn in eqs. (A6-A8).
It seems that system (A10)-(A14) holds well in the central region of the plasma and less well near the boundary; let us therefore consider the second-order expansion for small r.

From the normalization $T = p = 1$ at $r = 0$ we have from Spitzer-Ohm's law (A11):

$$B_\phi = \frac{r}{2} ; \qquad (A15)$$

introducing eq. (A15) into the pressure balance (A10) yields

$$p = 1 - \frac{1}{4} r^2 . \qquad (A16)$$

Introducing eq. (A16) and the ansatz

$$T = 1 - E\, r^2 \qquad (A17)$$

into eq. (A14) for the Lagrange density L yields two cases: either

$$E = 0.1 \qquad \mu_1 \; freely \; choosable , \qquad (A18)$$

or

$$\mu_1 = \frac{7}{3} \qquad E \; freely \; choosable . \qquad (A19)$$

Case (A19) gives negative α value and is not used in this paper.
Case (A18) yields

$$T = 1 - 0.10\, r^2 \qquad (A20)$$

and from the state equation $p = nT$

$$n = 1 - 0.15\, r^2 \qquad (A21)$$

or $T = n^{2/3}$; hence

$$\alpha = 0 \qquad at \qquad n = 1 . \qquad (A22)$$

Case (A22) is often observed in the stationary phase of IOC discharges.

Numerical computations yield approximately

$$\alpha \approx \alpha_{appr} = \frac{n\,(1-n)}{0.05+n} \left(\frac{0.1 - 0.14\, \mu_1}{1 - 0.5\, \mu_1} - \frac{0.10\, \mu_1\, (1-n)^2}{1 - 0.2\, \mu_1} \right) . \qquad (A23)$$

Replacing the parameter 0.05 by a big number, say 100, and $\mu_1 = 0$
and the parameter 0.1 by 130 in eq. (3.6) gives approximately the rule

$$\alpha \approx \alpha_{ap} = 1.3\, n\, (1-n) \qquad (6.5)$$

obtained from experimental findings. From this we learn that the theoretical boundary parameter 0.05 is much too small. This might have to do with the fact that sources and sinks are neglected in the theory.

Appendix B: Computer Program

We give here the part of the computer program which computes the

averaged experimental data	N(J), T(J) according to eq. (4.1)
at 20 equidistant meshpoints	R(J),
α according to eq. (3.5)	ALPHA = A(I,K) ,
the coefficients	C1, C2,
and the entropies (5.2) and (5.3)	SU $\sim S$ and SE $\sim S_e$.

R(J) is the radius of the flux surfaces in m;
JMAX = 20 corresponds to the ASDEX plasma radius $a = 0.4\ m$; (B1)
GW = length of the time integration interval = $2H + 1$ in eq. (4.3); HW=H+1;
GW = 7 in our plots.
ZEITQ = averaged time in ms.
The DO-5 loop contains the least-squares fit determination of c_1 and c_2 of

$$\alpha_{app} = c_1\, n + c_2\, n^2 \qquad (B2)$$

(see eq. (3.6)) with weight = GEW = 1-n for $R > 0.12$, GEW = 0 otherwise,
and, furthermore, the integrands of eqs. (5.2) and (5.3) for the entropies.
The DO-6 loop compares the experimental A(I,K) = α with the ansatz B(I,K)=α_{app} (see eq. (B2)),
the quantities U(I,K)=s and V(I,K)=$\alpha_{app}(n-1)/n$ which are proportional to the entropy per particle, and
the normalized experimental temperature Y(I,K)=T with Z(I,K)=$n^{2/3}exp(\alpha_{app}(1-1/n))$ (see eq. (3.5)).
The two-dimensional arrays are used for the plot routine.

In the following we present the program without input/output statements etc., furthermore, the ASDEX data used for the example $t = 2.03$ in Fig. 7 .

```
      .....
  DO 3       J=1,20
       R(J) = 0.02* J
      R2(J) = R(J) * R(J)
      R4(J) = R2(J)* R2(J)
3     R6(J) = R2(J)* R4(J)
         SE = 0.
         SU = 0.
        A11 = 0.
        A12 = 0.
        A22 = 0.
         B1 = 0.
         B2 = 0.
  DO 5       J=1,20
         ST = 0.
         SN = 0.
        NEC = 0.
        TEO = 0.
  DO 4       L=1,GW
        NEO = NEO+EXP( AON(L))
        TEO = TEO+EXP( AOT(L))
         ST = ST+ EXP( A1T(L)*R2(J) + A2T(L)*R4(J) + A3T(L)*R6(J))
4        SN = SN+ EXP( A1N(L)*R2(J) + A2N(L)*R4(J) + A3N(L)*R6(J))
        NEO = NEO / FLOAT( GW)
        TEO = TEO / FLOAT( 1000*GW)
       T(J) = ST  / FLOAT( GW)
       N(J) = SN  / FLOAT( GW)
       S(J) = ALOG( T(J)) - 0.666667 * ALOG( N(J))
      ALPHA = S(J) /( 1.- 1./N(J))
         SU = SU + S(J) * J * N(J)
         TE = TEO * T(J)
         NE = NEO * N(J)
         SE = SE + J*NE*( ALOG( TE) - 0.666667 * ALOG( NE))
  IF ( J. LE. 6)              GO TO 5
        GEW = 1.-N(J)
        A11 = A11 + GEW
        A12 = A12 + GEW* N(J)
        A22 = A22 + GEW* N(J)**2
         B1 = B1  + GEW* ALPHA/ N(J)
         B2 = B2  + GEW* ALPHA
5 CONTINUE
        DET = A11*A22 - A12*A12
      C1(I) = ( B1* A22 - B2* A12) / DET
      C2(I) = ( B2* A11 - B1* A12) / DET
         SP = 0.
  DO 6       J=7,20
          K = J-6
     X(I,K) = N(J)
     Y(I,K) = T(J)
     U(I,K) = S(J)
     A(I,K) = S(J) /( 1.- 1./N(J))
     B(I,K) = N(J)*( C1(I) + C2(I)* N(J))
     V(I,K) = (N(J)-1)*( C1(I) + C2(I) - C2(I) *(1.-N(J)))
     Z(I,K) = N(J)**0.666667 *EXP( V(I,K))
         SP = SP + (T(J) - Z(I,K))**2
6 PRINT 308, I,K
      .....
```

Part of Program

. . . . . .

Input Data

As an example, we present the coefficients A0N(M)... A3T(M) for the relaxed plasma state of shot no. 23349 at $t = 2.03\ s$, which are used in Figs. 6, 7 and 8.
The first column is the time in ms ; 1982 *to* 2082 is the time interval used in Sec. 3 for time averaging; the interval length of 100 ms corresponding to GW=7 is used for all plots in this paper.
The second column is $ln\ T_{e0}\ (eV)$;
the sixth column is $ln\ n_{e0}\ (10^{14}\ cm^{-3})$.
Large stochastic oscillations of the higher coefficients are found - nevertheless, the amplitude of the stochastic oscillations of the temperature and density are only about 3 - 10% of the temperature and density values.

Table B1: Coefficients for ASDEX shot no. 23349 at $t = 2.03\ s$.

2.03 SEC								
23349		7	2.03			IOC		
1982.6	6.90	-3.62	-103.0	167.8	-0.358	-7.19	-4.9	-179.4
1999.2	6.89	-5.79	-56.0	-4.2	-0.381	-4.95	-40.3	-59.7
2015.8	6.84	-3.48	-76.0	50.4	-0.466	-2.65	-60.8	-12.7
2032.3	6.89	-3.93	-87.0	110.6	-0.312	-7.70	2.7	-196.1
2048.9	6.91	-5.62	-44.7	-48.7	-0.433	-2.77	-69.1	27.4
2065.5	6.92	-3.42	-80.4	68.9	-0.354	-6.32	-27.3	-97.6
2082.0	6.88	-2.93	-89.4	104.6	-0.364	-7.96	3.8	-209.5
ZEIT	A0T	A1T	A2T	A3T	A0N	A1N	A2N	A3N

Appendix C: Safety Factor Ratio

In the case of circularly cylindrical geometry the safety factor ratio is defined by

$$\frac{q_a}{q_0} = \frac{1}{2\int_0^1 d\hat{r}\ \hat{r}\ j} \frac{B_a}{B_0}\ , \tag{C1}$$

with $\hat{r} = r/a$;
j = normalized current density component parallel to the axis,
B_a = toroidal magnetic field component at the plasma boundary,
B_0 = toroidal magnetic field component at the plasma centre.
If Spitzer conductivity

$$j = T^{3/2} \tag{C2}$$

and small plasma β

$$B_a = B_0 \tag{C3}$$

are assumed, we have

$$\frac{q_a}{q_0} = \frac{1}{2\int_0^1 d\hat{r}\ \hat{r}\ T^{3/2}}\ . \tag{C4}$$

Inserting $T = exp(\frac{2}{3}\ U\ \hat{r}^V)$ into eq. (C4) with $+\infty$ instead of 1 as upper integration limit yields exactly

$$\frac{q_a}{q_0} = \frac{P\ U^C}{\Pi(C)}\ ; \tag{C5}$$

this can be obtained by introducing $X = \frac{2}{3}\ U\ R^V$ as integration variable instead of R. P and C are defined in eq. (7.8). Equation (C5) is the main part of eq. (7.7) for q_a/q_0. Furthermore, eq. (7.7) contains the factor

$$\frac{1}{1\ -\ e^{-P}}\ , \tag{C6}$$

which arises if the correct integration limit 1 is used in eq. (C4) instead of ∞. Factor (C6) exactly desribes the Gauss case $V = 2$; otherwise factor (C6) is only approximately valid, the inaccuracy being a few per cent.

In the range of interest $-0.5 \leq C \leq 0$ the factorial can be approximated by

$$\Pi(C) = \int_0^\infty dX\ X^C\ e^{-X} \approx \frac{1}{1+C} - 0.43\ C - 0.1\ C^3\ , \tag{C7}$$

the inaccuracy is about 0.001 .

Appendix D: Explanations, Auxiliary Computations, etc.

Re. eq. (1.1) Water Glass Entropy

Given:
two water glasses
with temperatures

$T_1 = T_0 - \Delta T$
$T_2 = T_0 + \Delta T$,

heat flux proportional to
the temperature difference

$$\frac{d\Delta T}{dt} = \frac{\Delta T}{2\, t_{rel}} .$$

Solution:

$$\Delta T = \Delta T_0 \, exp(-\frac{t}{2\, t_{rel}}) .$$

Entropy:

$$S = \int(dQ_1/T_1 + dQ_2/T_2)$$
$$S = b \int(dT_1/T_1 + dT_2/T_2)$$

$$S = b \left(ln(T_0 - \Delta T) + ln(T_0 + \Delta T) \right) ,$$

development for $\Delta T/T < 1$:

$$S = S_0 - b \left(\left(\frac{\Delta T}{T_0} \right)^2 + \frac{1}{2} \left(\frac{\Delta T}{T_0} \right)^4 + \ldots \right) .$$

Cut-off after the second-order term and inserting the exponential for ΔT yields eq. (1.1).

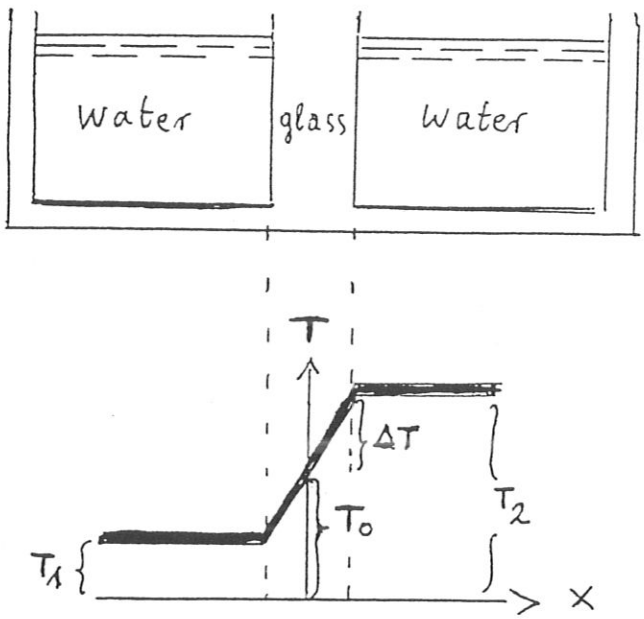

Fig. 15
Two water glasses
and their temperature

Re. eq. (2.2) Entropy per Particle

Given: N particles in a volume V.

Then we have:

particle density $n = N/V$

state equation $pV = N\,kT$

. $p = n\,kT$

Normalization $p = T = n = 1 \qquad at\ r = 0$

Boltzmann const $k = 1$

total energy $U = pV\ /\ (\gamma - 1)$ (Feynman lectures, eq.(39.11))

energy conservation $dU = dQ - p\,dV$

verbal: the total energy U increases by addition of heat dQ and by compression $-\,p\,dV$.

Def. of entropy: $dS = dQ\ /\ T$

special: isotherm: $dU = 0$

. $dS = p\,dV/(pV/Nk)$

. $S = Nk\,ln\,V + f(T)$

special: adiabatic: $S = const$

. $dQ = 0$

. $dU + p\,dV = 0$

. $p\,dV + V\,dp + (\gamma - 1)\,p\,dV = 0$

. $dp/p + \gamma\,dV/V = 0$

. $p\,V^{\gamma} = const$

. $T\,V^{\gamma-1} = const$

Hence

1.) S must be $= Nk\,ln\,V + f(T)$

2.) S must be a function of $T\,V^{\gamma-1}$;

hence for $k = 1$ we have

$$s = \frac{S}{N} = s_0 + \frac{ln(T\,n^{1-\gamma})}{\gamma - 1} \qquad (2,2)$$

Acknowledgements

The author is grateful to D. Pfirsch, F. X. Soeldner and the ASDEX team for valuable discussions.

References

/1/ D. Pfirsch and F. Pohl, Plasma Physics and Controlled Fusion, **29**, 697, (1987)
/2/ D. Pfirsch and F. Pohl, Z. Naturforsch. **43a**, pp.395-401 (1988)
/3/ H. Roehr et al., IPP III/121 June 1987
/4/ F. X. Soeldner et al. Phys. Rev. Letters **61**, 1105 (August l988)
/5/ F. X. Soeldner et ASDEX team, private communication
/6/ F. X. Soeldner et al., IAEA Technical Committee Meeting on Pellet Injection
. and Toroidal Confinement, Ising 1988
/7/ F. X. Soeldner et ASDEX team, private communication
. IPP Monatliche Mitteilungen August 1988
/8/ F. X. Soeldner et al.,
. 16^{th} European Conference on Controlled Fusion and Plasma Physics,
. Vol. I, p. 187, Venice, Italy, March 13-17, 1989
/9/ B. Coppi, Comments Plasma Phys. Contr. Fusion **5**, 261, (1980)
/10/ The Feynman lectures on physics, R. Oldenbourg Verlag Bilingua
. Muenchen Wien 1973